Final Technical Report

Award Number: G11AP20120

Understanding Strain Fluctuations Before And After The El Mayor/Cucapah Earthquake

Start and End Dates: March 1, 2011 to July 31, 2012

Duncan Carr Agnew
Institute of Geophysics and Planetary Physics
Scripps Institution of Oceanography
University of California
La Jolla CA 92093-0225 USA
(858) 534-2590 (FAX 534-5332)
dagnew@ucsd.edu

March 6, 2013

Abstract

This grant supported the analysis of strainmeter and other data related to the El-Mayor Cucapah earthquake of 2010:094. An examination of the seismicity indicates that three unusual "bursts" occurred along the Elsinore fault zone in the month before the mainshock, at distances well away from the epicenter. These do not appear to have been accompanied by any unusual deformation signals; but immediately after the mainshock large rates of strain were seen on most of the longbase strainmeters, indicating both afterslip on the main rupture and shallow triggered creep on the southern San Andreas fault. These rates decayed over the following days at most sites; however, the three strainmeters at PFO showed abrupt changes in rate a few hours after the mainshock, in a pattern consistent with post-seismic strains from the Anza shock of 2005. Inversion of these data show that the slip that caused these strains must have been at seismogenic depths on the San Jacinto fault at the southeast end of the Anza seismic gap. If we assume both events were at the same depth, the moment release in both 2005 and 2010 was 1.8×10^{17}N-m, equivalent to magnitude 5.5, with a duration of about 50 days.

1 Introduction

One of the hopes of the Plate Boundary Observatory project was that a large earthquake would provide signals during its 15-year lifespan. This was by no means assured, since Monte Carlo simulations (using observed seismicity) showed that in the first few years of operation there was only a 50% chance of two or more PBO GPS stations seeing a coseismic signal of more than 100 mm.

However, sometimes even the improbable happens: in 2010 there occurred the first large earthquake of the 21st century in southern California: the El-Mayor/Cucapah shock (M_w 7.2), which occurred on 2010:094:022 when over 100 km of fault ruptured, almost all south of the international border. This earthquake means that the PBO has data from the sixth largest earthquake in the last 100 years on the transform part of the Pacific/North-America plate boundary. The US border has meant that the instrumental coverage was fairly one-sided, but these records still represent an unequaled amount of crustal deformation data for a large earthquake on this plate boundary.

The El-Mayor/Cucapah (hereafter EMC) earthquake is named for the two mountain ranges it occurred in; these divide the Mexicali Valley from another large area below sea level to the west, Laguna Salada. The main plate boundary runs along the Cerro Prieto and Imperial faults in the Mexicali and Imperial valleys to the NE, but some slip is transferred to the SW, and the faults along the west side of the mountain ranges are assumed to connect to the Elsinore fault to the northwest. Slip rates for the Elsinore fault zone, including this portion south of the border, are generally estimated to be a few mm/yr; the strain rate found by Savage *et al.* (1994) across Laguna Salada was less than $10^{-7}\mathrm{yr}^{-1}$, with a significant component of EW extension, not seen further north or south. A relatively fresh scarp found by Mueller and Phillips (1995) along the western side of the mountains, called the Laguna Salada fault, is generally assumed to be associated with a large earthquake (magnitude 7.2) in February 1892; the intensity reports are at least consistent with such a location (Hough and Elliot, 2004).

Just over 118 years later, the EMC earthquake (magnitude 7.2) was also caused by rupture of a fault in the mountains, though the surface rupture is separate from the one that has been associated with the 1892 shock.

An immediate foreshock sequence in the region of the EMC epicenter began a few hours before the mainshock. The mainshock appears to have been a somewhat complex event, with an initial rupture around the epicenter (in the Sierra El Mayor) followed about 15 s later by slip running NW along the west edge of the Sierra Cucapah to about its northern end, and the US border; there is good evidence (Wei *et al.*, 2011b) that faulting also extended well to the SE of the epicenter. The extent of the aftershocks suggests that faulting extended north of the border, but only small amounts of surface rupture were observed there. Surface rup-

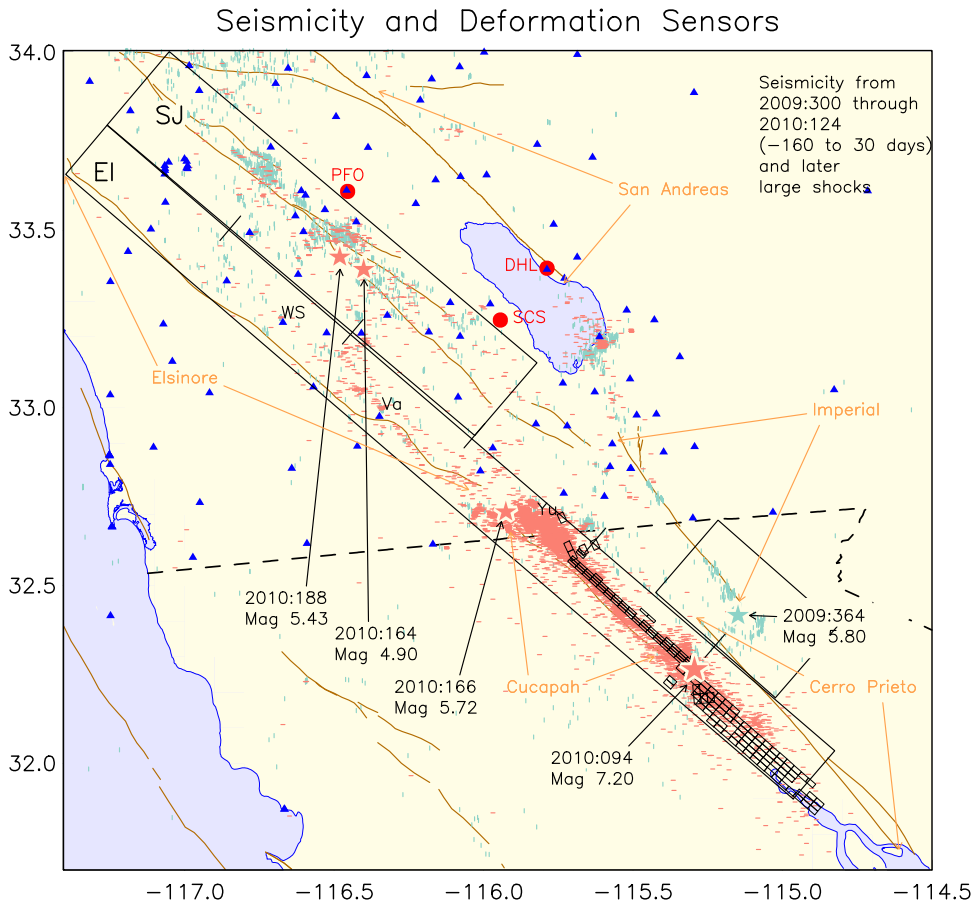

Figure 1: Map showing the seismicity immediately before (green) and after (reddish) the EMC earthquake, superimposed on known faults. Also shown are continuous GPS stations (blue triangles), and longbase strainmeters (red disks with labels) The two boxes are used to separate seismicity on the Elsinore fault (**El**) from that on the central San Jacinto fault (**SJ**); see Figure 2. Tics on boxes are at 50 km intervals.

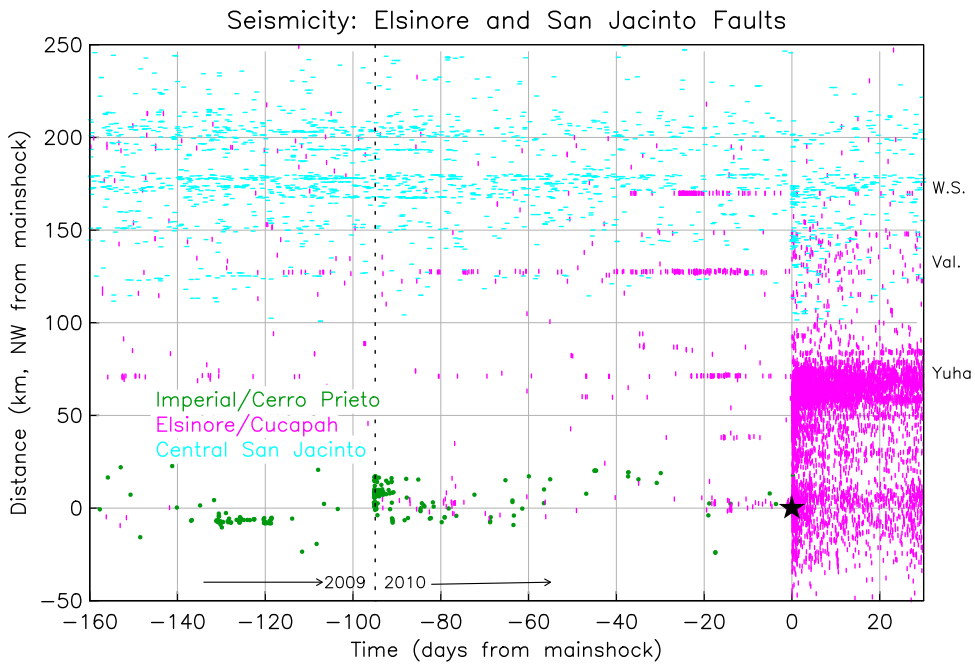

Figure 2: Seismicity along the Elsinore and San Jacinto faults, plotted against time and distance along the faults (on the axis defined in Figure 1, with zero distance at the EMC epicenter. Magenta marks are earthquakes in box **El** of Figure 1; cyan marks are earthquakes in box **SJ**. **WS** is the Warner Springs cluster, **Va** the Vallecito cluster, and **Yu** the Yuha cluster.

ture has been mapped along the northern part of the Sierra Cucapah, with both strike-slip and vertical motion. Initial reconnaissance did not observe rupture further south, although cross-correlation of satellite images does indicate several meters of horizontal displacement along a sharp boundary south to the epicenter and beyond.

2 Work Plan and Results

This section describes our investigations in three areas: evidence for unusual activity in the Elsinore fault zone before the earthquake; immediate postseismic strains and their interpretation; and evidence for triggered aseismic slip, possibly still ongoing, in the Anza region of the San Jacinto fault zone.

Name	N	Centroid		Area	Depth		Vol
		Lat	Long		Mean	Range	
Warner	108	33.2540	−116.6790	0.105	6.91	1.31	0.14
Vallecito	350	32.9980	−116.3411	1.73	7.85	2.98	5.2
Yuha	168	32.7277	−115.8283	2.58	5.57	3.69	9.5

Table 1: Parameters of seismicity bursts. N is the number of events. The area is in km^2 and the volume in km^3.

2.1 Pre-Earthquake Bursts on the Elsinore Fault

This earthquake was preceded and followed by interesting seismicity patterns, which are yet another illustration of Clarence Allen's classic statement that all large earthquakes are preceded by interesting seismicity patterns, each one different. Figure 1 is a map view of seismicity around the time of the EMC earthquake, while Figure 2 plots earthquakes as a function of time and distance along faults.

In hindsight the foreshock sequence for the EMC earthquake began 95 days before it, with a magnitude 5.8 shock at the southern end of the Imperial fault on 2009:364, which was followed by an aftershock sequence, shown in green in Figure 1 and in brown in Figure 2.

But the seismicity we focus on here was later and more distant (Figure 2. About 30 days before the mainshock, three small areas along the Elsinore fault zone produced bursts of seismicity. The southernmost one was at the north end of the region that subsequently ruptured, though the amount of mainshock slip in this area was small. The other two are 125 and 170 northwest of the epicenter. Table 2.1 gives the parameters of these seismicity bursts. None occupy a large volume; the Warner Springs cluster is extremely tight, with epicenters in a region less than 300 m square, and a source volume well under a cubic kilometer.

Figure 3 shows the time history of seismicity in these three areas. The northernmost burst, near Warner Springs, shows essentially no activity before 2010; the other two occasionally show temporally-clustered shocks, but nothing like the sequence prior to the EMC earthquake. The bursts in 2010 included the largest events for each cluster: magnitude 3.5 for the Warner Springs cluster, 4.1 for the Vallecito cluster, and 2.9 for the Yuha cluster,

These bursts, while reminiscent of the precursory swarms noted by Hauksson *et al.* (1995) before the Northridge earthquake, are more tantalizing because they occurred on the same fault as the subsequent mainshock – though the distance between the seismicity bursts and the eventual mainshock is too large for static stress triggering to play an obvious role. While clustered activity has occurred at other times along the Elsinore fault, Vidale and Shearer (2006) show only one temporally-compact burst on this fault from 1984 through 2006. Given

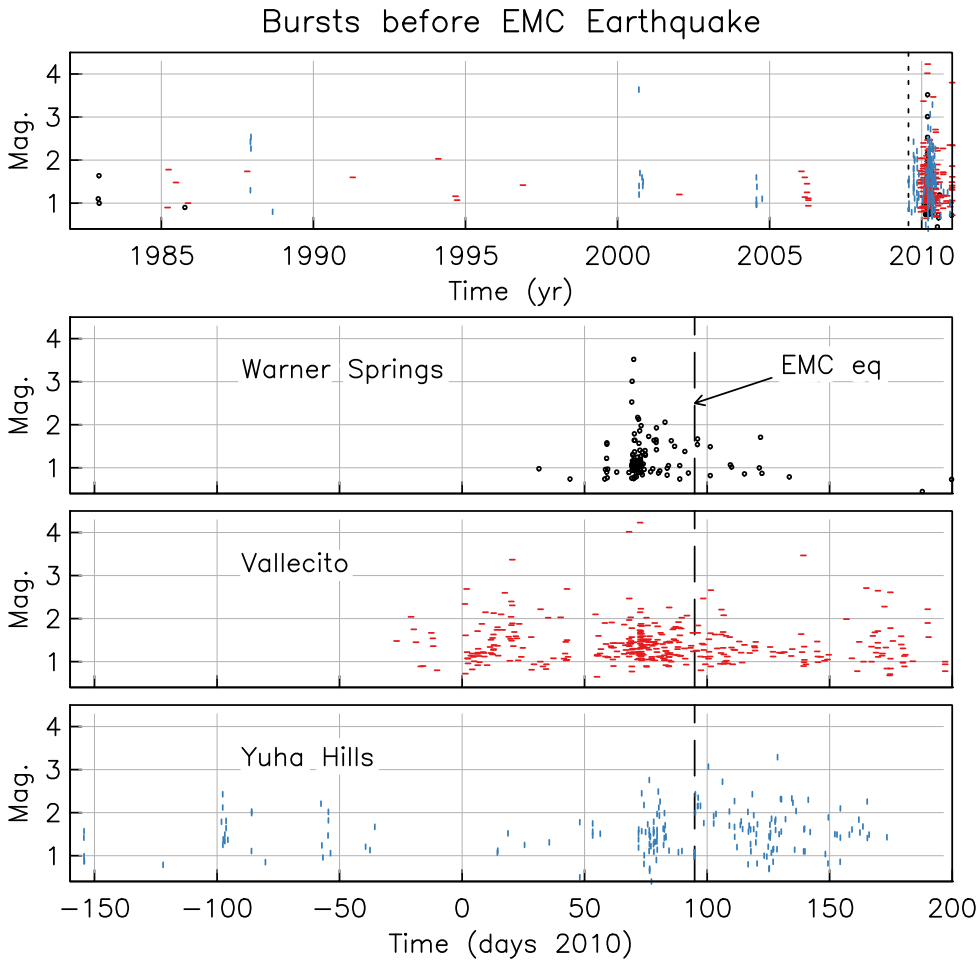

Figure 3: Time history of seismicity in the three burst areas, plotted as magnitude against time. The top frame shows the activity over the entire span from 1981 through mid-2011. The next three frames show the activity in each burst, using the same symbols and colors as in the top frame.

the pitfalls in testing a hypothesis that we create from the data (Heaton, 1975, 1982) it is difficult to see how the significance of this behavior could be reliably established. So these bursts must be characterized as suspiciously unusual, but enigmatic. It would of course be tempting to suspect them of being triggered by a large-scale precursory strain – except that no strain transient is seen on any of the laser strainmeter data at the start of these events. Less problematically, Figure 2 shows that, after the mainshock, seismicity increased along the Elsinore and San Jacinto faults as far as 100 km from the northern end of the main aftershock zone; this increase has decayed at the same rate as the main aftershocks. This seismicity at least suggests the possibility of triggered slip at seismogenic depths on these faults, something that, as we describe in Section 2.3, is also suggested by some of the laser strainmeter data.

2.2 Immediate Postseismic Strains

Figure 4 shows the immediate response on the seven longbase strainmeters that were relatively close to this earthquake. All the strainmeters operated throughout the event, but the recordings have unreliable intervals because of the equivalent of a GPS "cycle slip". The strains from the largest seismic waves were large enough that the laser beams for these instruments were no longer pointed accurately at the far end; when this happens the interference pattern degrades and strain is not measured for several minutes. In the plots we have set the coseismic offset to be zero across this gap. Since information on coseismic behavior is available from seismic, GPS, and InSAR, not having this signal from the longbase strainmeters for such large events, while unfortunate, is actually not too great a loss. We do have reliable estimates of coseismic offsets from the EW longbase tiltmeter at PFO, and from the more distant strainmeters in Los Angeles and Cholame.

After the interruption from strong shaking the strainmeters again give continuous records of deformation to very high accuracy. Figure 4 shows 1-Hz data, lowpassed above 0.01 Hz to remove the seismic coda. These records show immediate, relatively smooth, high-rate strain changes: postseismic deformations, presumably caused by afterslip on the fault. The relative sizes of this deformation at SCS and DHL are comparable to the ratios of coseismic strains computed from a model, so such a source is very plausible. There is an enhanced response at DHL; we believe this is the result of triggered creep on the nearby San Andreas fault. Creep was subsequently observed over large stretches of the fault trace by Wei *et al.* (2011a). The recordings at DHL match short-term strain changes (time spans of a few minutes, sometimes in groups over one to seven daya) that we have observed in 1999, 2003, 2006, and 2008 – though none of these were at times of strong ground motions, and themselves appear to be entirely aseismic.

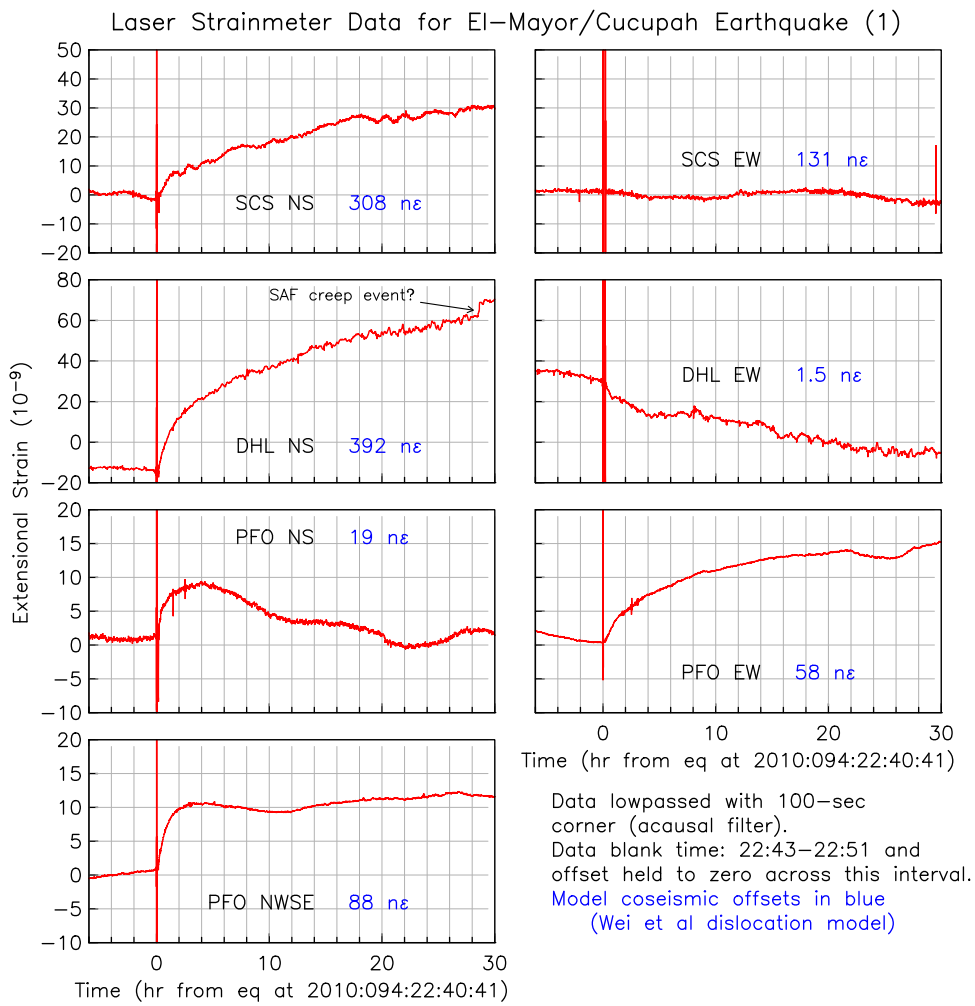

Figure 4: Strain on all the long-base strainmeters close to the EMC earthquake (see 1 for locations). Time runs from 6 hr before the earthquake to 30 hr after. All data have been smoothed with a FIR filter with a corner frequency of 0.01 Hz (to remove the coda); as explained in the text, there is no reliable data at the time of strongest shaking, and the strain change during this period has been set to zero for clarity. The value in blue in each plot is the coseismic strain predicted by the model of Wei *et al.* (2011b).

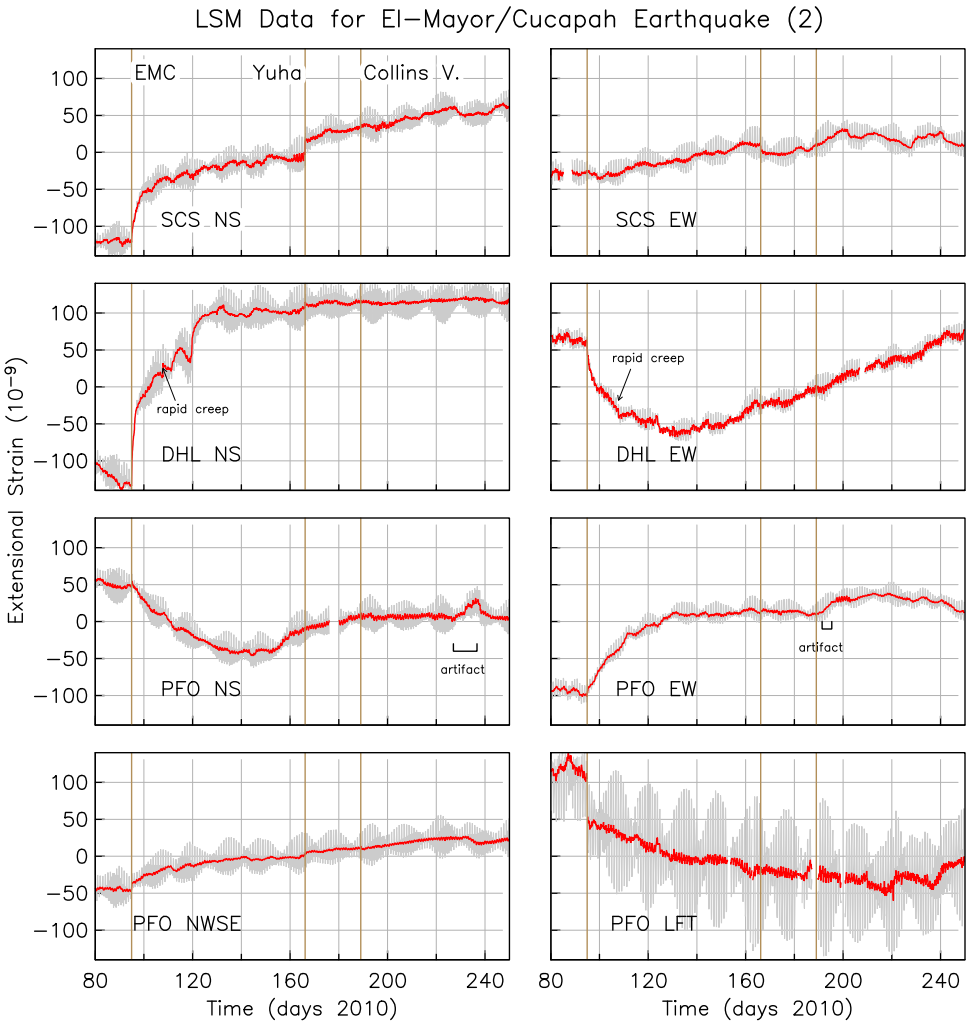

Figure 5: Strain on all the long-base strainmeters close to the EMC earthquake (see 1 for locations), from about 2 weeks before to 4 months after the earthquake. Heavy lines show hourly data with tides removed; the full record (tides included) is underplotted in gray. Brown vertical lines are times of larger earthquakes.

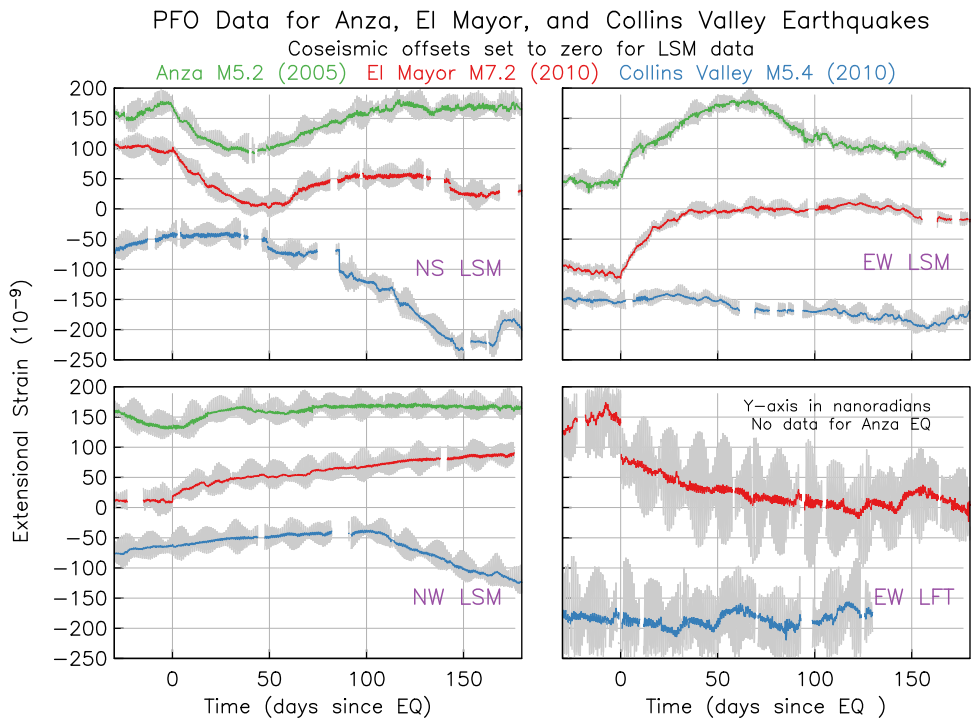

Figure 6: Strain on the long-base strainmeters and EW long-base tiltmeter at PFO for three earthquakes. Heavy lines show hourly data with tides removed; the tidal data is underplotted in gray. The red line is for the EMC earthquake, the green line for the 2005 Anza event, and the blue line for the Collins Valley earthquake of 2010. (The locations of all these shocks are shown on Figure 1). Because the tiltmeter measures absolute tilt, its time series can include the coseismic offset.

2.3 Triggered Slip on the San Jacinto Fault?

As Figure 4 and Figure 5 both show, the postseismic strain changes at PFO, closest to the San Jacinto fault is more complicated than for the other strainmeters. All three PFO strainmeters start by showing postseismic strains that are roughly consistent, in size and shape, with their source being afterslip on the just-ruptured fault: the signals are of the same sign, and larger on the NWSE and the EW than on the NS. But soon after, the strain rate on the NS changes sign, while that on the NWSE falls to near zero.

Over the first month after this earthquake (Figure 5) the NS and EW show trends of about the same size but opposite sign, while the NWSE shows generally less change; we also observe a significant change in trend on the long fluid tiltmeter. After this, the strain rates on both the NS and EW slow down, while the NWSE shows persistent extension, the NS and EW change sign – to an extent that the postseismic strain is nearly recovered

This pattern of strain changes is something we have seen before, following the M_w 5.2 Anza

earthquake on 2005:163. Figure 6 shows this by plotting the strains around the time of both earthquakes, with the x-axis in terms of time from the event.[1]

The similarity in strain signals in 2010 and 2005 is obvious. One concern might be that this similarity might be caused by the response of the site to strong shaking from any source, rather than being a measure of strains over a wider area. Fortunately we have several strands of evidence to rule this out. Figure 6 shows one, namely the strains around the time of the Collins Valley earthquake (M_w 5.4) on 2010:189. This earthquake was southeast of the 2005 event (both are shown in Figure 1), and somewhat further from the mapped trace of the San Jacinto fault. It produced shaking at PFO that was comparable to that from the 2005 shock, but without causing a long-term response on the strainmeters.

While it might not seem feasible to find the source of this slip from only three records, this turns out to be possible. The important point is that for slip in one location the ratio of observed strains does not vary. Recognizing that we measure strain change, we denote the rate of strain on the i-th instrument (of N total) by $\dot{\epsilon}_i$. Define the unit vector $\hat{\mathbf{a}}(t)$ whose components are:

$$\hat{a}_i(t) = \frac{\dot{\epsilon}_i(t)}{\sqrt{\sum_{i=1}^{N}(\dot{\epsilon}_i(t))^2}} \qquad \text{for} \quad i = 1,\ldots,N \tag{1}$$

Now consider slip $s(t)$ at location $\mathbf{x}$; we expect that the strain rate on the i-th instrument will be given by

$$G_i(\mathbf{x})\dot{s}(t) \qquad \text{for} \quad i = 1,\ldots,N \tag{2}$$

where $\dot{s}$ is the slip rate at a location $\mathbf{x}$, and $G_i(\mathbf{x})$ is the Green function relating slip at location $\mathbf{x}$ to strain on the i-th instrument. Define a second unit vectors $\hat{\mathbf{b}}(\mathbf{x})$ whose components are

$$\hat{b}_i(\mathbf{x}) = \frac{G_i(\mathbf{x})}{\sqrt{\sum_{i=1}^{N}(G_i(\mathbf{x}))^2}} \qquad \text{for} \quad i = 1,\ldots,N \tag{3}$$

If the strains are actually given by equation (2), then computing $\hat{\mathbf{a}}$ will give $\hat{\mathbf{b}}$; the slip rate $\dot{s}(t)$ in equation (2) will cancel, making $\hat{\mathbf{a}}$ and $\hat{\mathbf{b}}$ equal; since they are unit vectors, this amounts to saying that they will point in the same direction in N-dimensional space. Given an observed $\hat{\mathbf{a}}$, we can then find the misfit between this and the relative strains for slip at $\mathbf{x}$ by finding the dot product of the two unit vectors, which gives us the angle between them. A suitable measure of misfit is

$$m(t,\mathbf{x}) = 1 - \arccos(\hat{\mathbf{a}} \cdot \hat{\mathbf{b}}) \tag{4}$$

which will be zero when $\hat{\mathbf{a}}$ and $\hat{\mathbf{b}}$ have the same direction.

[1] In interpreting these data, it should be remembered that the NS strainmeter is only partly anchored. Also, certain sections of the data (shown without the tidal background but with a colored straight line) have been skipped because of problems with miscounting electronics.

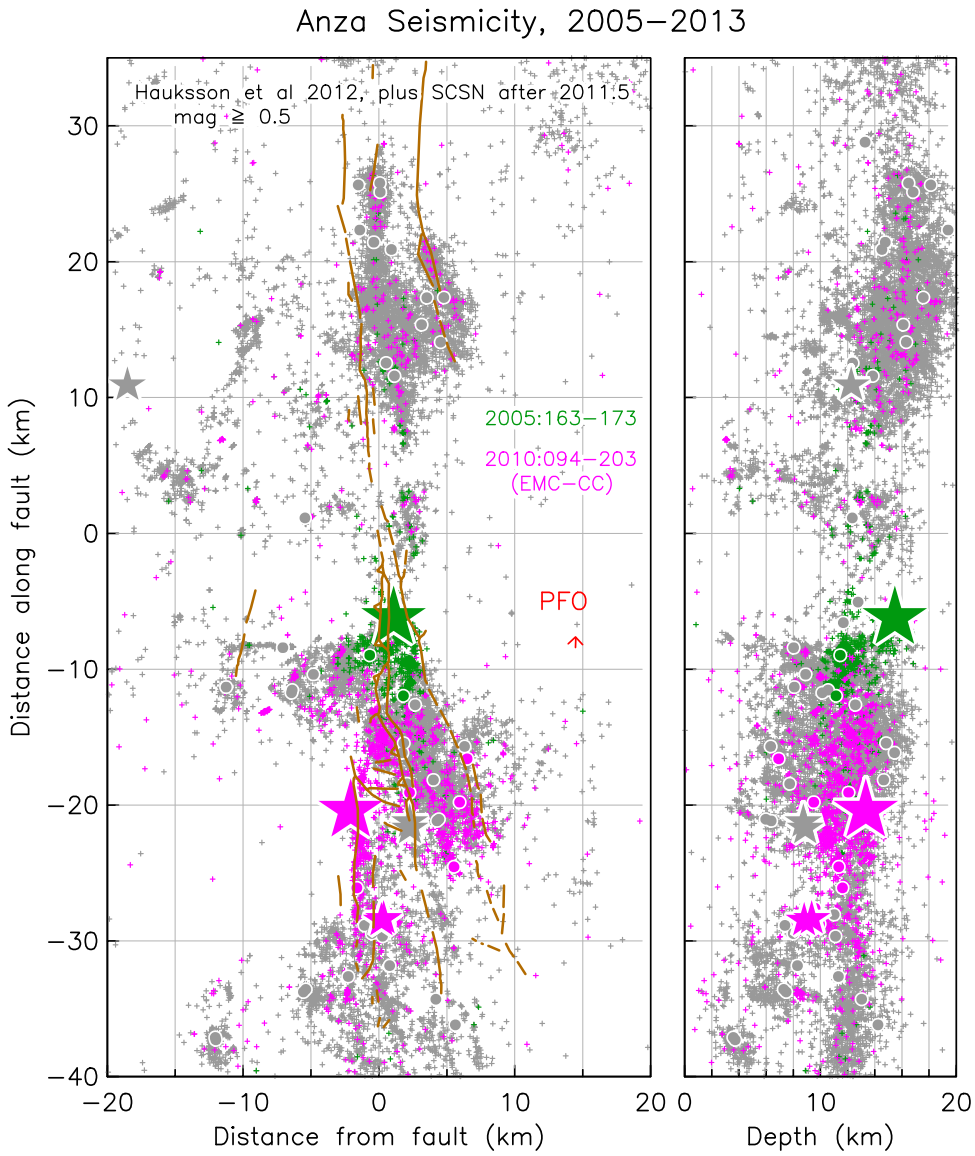

Figure 7: Seismicity of the Anza region near PFO (laser strainmeters shown to scale). The projection used in the map view (left) is an Oblique Mercator striking 43° through 33.5640°N, 116.6266°W (where Highway 371 crosses the fault). The cross-section on the right projects all earthquakes to this central meridian. Pluses are magnitude less than 3, circles magnitude 3 to 4, small stars 4 to 5, and large stars greater than 5. Green is for the Anza event of 2005:163 and aftershocks within 10 days of it; magenta is for earthquakes after the El Mayor shock of 2010:094 and running until 15 days after the Collins Valley shock of 2010:188. Gray is all other shocks from the start of 2005 until 2011:181 (the end of the catalog by Hauksson *et al.* (2012)) which the hypocenters are taken from.

Event	Time	Strain, 10^{-9}		
	(d)	NS	EW	NWSE
Anza 2005	45	−70	120	30
EMC 2010	50	−100	100	50

Table 2: Postseismic strains following the 2005 Anza and 2010 El Mayor earthquake, estimated from Figure 6.

So given the strain rates as a function of time, or the strain over some time span, we can find, for each time, $m(\mathbf{x})$, the minimum of which will give the source location that best agrees with the relative rates of strain. The slip rate assuming this source location is then given by

$$\dot{s} = \frac{\sqrt{\sum_{i=1}^{N}(\dot{\epsilon}_i(t))^2}}{\sqrt{\sum_{i=1}^{N}(G_i(\mathbf{x}))^2}} \tag{5}$$

To apply this to slip on the San Jacinto fault in the Anza area, (whose seismicity we show in Figure 7, we assume that the slip is right-lateral. Computing the strains induced at PFO by slip on different parts of the San Jacinto fault (represented by a plane dipping at 82° gives a set of unit vectors $\hat{\mathbf{b}}$ which we can compare with unit vectors $\hat{\mathbf{a}}$ estimated from the strain changes after the 2005 Anza and 2010 EMC earthquakes. We estimate the net changes over a longer period using Figure 6, with values given in Table 2. The results are shown in Figure 8, in which the colored areas show the acceptable regions: (an angle between unit vectors of 15° or less, or $m < 0.035$). This plot shows that only a small region on the fault can produce strain changes with the observed ratios. Since the ratios are similar for the two cases, it is not surprising that the acceptable regions are in roughly the same place – though the slip in 2005 is much less constrained in depth than that in 2010.

If we take the fault-plane location that minimizes the angle between $\hat{\mathbf{a}}$ and $\hat{\mathbf{b}}$, we can find the total slip – or more correctly, the moment release, since we do not know the size of the source. For the 2005 aseismic strain, the moment released is 1.8×10^{17}N-m (equivalent to $M_w = 5.5$; for the 2010 strains, the value is also 1.8×10^{17}N-m. This assumes that the source areas were at the same depth; the absolute best-fitting source region for the 2005 event is actually at 20 km depth, which would make for a source about four times as large (equivalent magnitude 5.9). The sources equivalent to a magnitude 5.5 event produce a maximum of 1.6 mm horizontal displacement and 2.0 mm vertical displacement on the nearest continuous GPS stations – though most of these available in 2010 were not in place in 2005. The results of blind tests of detection methods (sponsored by SCEC), show that motions of this size and duration would be undetectable.

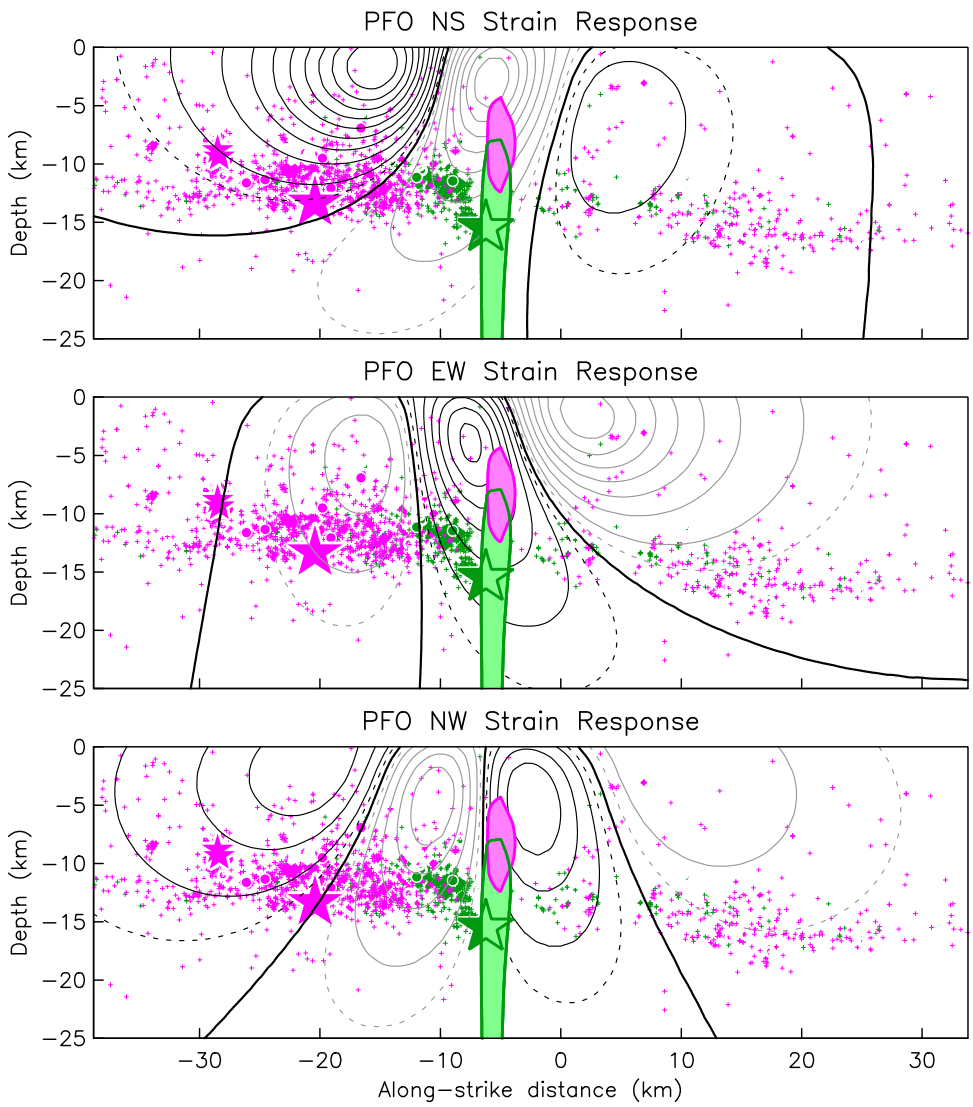

Figure 8: View of the San Jacinto fault, using the same coordinates (and colored seismicity) as in Figure 7. The two colored regions show the regions in which right-lateral slip would produce strain changes with the ratios derived from the values in Table 2.

3 Summary

The strainmeter data around the time of the El Mayor/Cucapah earthquake show several signals of interest. The first is actually a signal that does *not* appear, namely any strain changes to accompany the seismicity bursts described in Section 2.1. Without this well-determined null, it would be very tempting to imagine that these bursts were caused by some kind of pre-seismic strain acceleration. Next, the strainmeters provide the most detailed record of the immediate postseismic changes, including triggered shallow slip on the San Andreas fault. And most interestingly, the PFO strain records provide strong evidence for aseismic slip in the Anza gap, both after the 2005 Anza earthquake, and (with a few hours delay) after the 2010 EMC earthquake.

References

Hauksson, E., L. M. Jones, and K. Hutton (1995), The 1994 Northridge earthquake sequence in California: seismological and tectonic aspects, *J. Geophys. Res.*, **100**, 12,335–12,355.

Hauksson, E., W. Yang, and P. Shearer (2012), Waveform relocated earthquake catalog for Southern California (1981 to June 2011), *Bull. Seismol. Soc. Amer.*, **102**, 2239–2244, doi: 10.1785/0120120010.

Heaton, T. H. (1975), Tidal triggering of earthquakes, *Geophys. J. Roy. Astron. Soc.*, **43**, 307–326.

Heaton, T. H. (1982), Tidal triggering of earthquakes, *Bull. Seismol. Soc. Am.*, **72**, 2181–2200.

Hough, S. E., and A. Elliot (2004), Revisiting the 23 February 1892 Laguna Salada earthquake, *Bull. Seismol. Soc. Am.*, **94**, 1571–1578.

Mueller, S., and R. J. Phillips (1995), On the reliability of lithospheric constraints derived from models of outer-rise flexure, *Geophys. J. Internat.*, **123**, 887–902.

Savage, J. C., M. Lisowski, N. E. King, and W. K. Gross (1994), Strain accumulation along the Laguna Salada fault, Baja California, Mexico, *J. Geophys. Res.*, **99**, 18,109–18,116.

Vidale, J., and P. Shearer (2006), A survey of 71 earthquake bursts across southern California: Exploring the role of pore fluid pressure fluctuations and aseismic slip as drivers, *J. Geophys. Res.*, **111**, doi:10.1029/2005JB004034.

Wei, M., D. Sandwell, Y. Fialko, and R. Bilham (2011a), Slip on faults in the Imperial Valley triggered by the 4 April 2010 Mw 7.2 El Mayor/Cucapah earthquake revealed by InSAR, *Geophys. Res. Lett.*, **38**, L01,308, doi:10.1029/2010GL045235.

Wei, S., *et al.* (2011b), Superficial simplicity of the 2010 El Mayor-Cucapah earthquake of Baja California in Mexico, *Nature Geosci.*, **4**, 615–618, doi:10.1038/ngeo1213.